Cauer Ladder Network with Constant Basis Functions for Eddy Current Problems Involving Conductor Movement

Kengo Sugahara[1], Naoto Tanimoto[1], Yasuhito Takahashi[2], and Tetsuji Matsuo[3]

[1]Graduate School of Science and Engineering, Kindai University, Osaka, Japan, ksugahar@kindai.ac.jp
[2]Department of Electrical Engineering, Doshisha University, Kyotanabe, Japan, ytakahashi@mail.doshisha.ac.jp
[3]Graduate School of Engineering, Kyoto University, Kyoto, Japan, matsuo.tetsuji.5u@kyoto-u.ac.jp

This article proposes a Cauer ladder network with constant basis functions for eddy current problems involving translational movements. The analysis domain is decomposed into two domains: the stator part and the mover part. The Cauer ladder network method is applied to each domain to derive circuit parameters and corresponding basis functions to reconstruct the eddy current and compute the Lorentz force. Interactions between the two domains are modeled by current-controlled voltage sources connected to each stage of the Cauer ladder network. The gains of the current-controlled voltage sources are computed by numerical integration of the vector potential induced by the coil. An analysis of the TEAM Workshop Problem 28 was performed, and the results were validated by comparing them with those obtained by the commercially available software and showed a significant reduction in computational time.

***Index Terms*—Cauer ladder network, eddy currents, model order reduction, levitation devices, TEAM 28**

I. Introduction

THE finite element method has been widely used for analyzing electric machines because nonlinear magnetic effects and translational movements can be accurately modeled along with the governing mechanical equations. However, the finite element method is time-consuming, especially when real-time control systems are simulated. An efficient approach to reduce the computational cost of the finite element method is model order reduction (MOR), and various researches are carried out on this topic [1]–[4].

We have been conducting research on one of the MOR methods, i.e., the Cauer Ladder Network (CLN) method [5]–[9]. The CLN method is a method to represent the magnetic field by a ladder-type circuit composed of inductors and resistors and electromagnetic fields are expanded with the corresponding electromagnetic field modes. In this paper, we propose a method to use constant basis functions that do not change with the movement of themover in the CLN method for eddy current fields involving a mover. A method to use parameterized basis functions with respect to the movement of the mover was proposed in [10], [11]. When using parameterized basis functions with respect to the movement of the mover, it is necessary to limit the space where the mover moves in advance and construct the CLN circuit within that range. Moreover, there is a disadvantage that the implementation on the circuit simulator becomes complicated when the time derivative of the circuit parameters or the corresponding basis function is required. When using the proposed method, both circuit parameters and basis functions are constant, so the implementation on the circuit simulator is simple and analysis can be easily performed with Simulink and other tools that are commonly used for control design.

In this paper, we deal with one of the simple examples of eddy current fields involving a mover, the TEAM Workshop Problem 28 (TWP28) [11]–[13].

II. Cauer ladder network extraction

TWP28 [12] was chosen as an example because it provides a simple model to build the proposed formulation. However, we can extend it to multiple-conductor problems by introducing a multi-port CLN [14] with multiple controlled sources.

Fig. 1 shows the model geometry of TWP 28. The moving aluminum plate is non-magnetic and has $\sigma = 34\ \mathrm{MS/m}$ conductivity. Two concentric coils are connected in anti-series, and are placed below the aluminum plate, and carry a sinusoidal current with $I = 20\mathrm{A}$ amplitude and $f = 50\mathrm{Hz}$ frequency. The inner and outer coils have 960 and 576 turns, respectively. The gap between the aluminum plate and the coils, z_{GAP}, varies from 3.8 mm to 20 mm.

In this formulation, the problem is decomposed into two models: (a) current sources and (b) moving aluminum plate, as shown in Fig. 1. The solutions of each model are superposed to reconstruct the solution of the original problem. For the simplicity, we assume the strand current in thr current sources in Fig. 1 (a), and ignore the eddy currents. Hence, the source vector potential, denoted as

Manuscript received December xx, 20xx; revised August xx, 20xx. Corresponding author: K. Sugahara (email: ksugahar@kindai.ac.jp).

$\boldsymbol{A}_s$, by the current can be computed analytically. In Fig. 1 (b), the governing equation of the aluminum domain is formulated as reduced problems (1), truncated with the infinite elements.

$$\nabla\times\left(\frac{1}{\mu}\nabla\times\boldsymbol{A}_r\right)+\sigma\frac{\partial}{\partial t}\boldsymbol{A}_r=-\sigma\frac{\partial}{\partial t}\boldsymbol{A}_s(z_{\mathrm{gap}}(t),t) \quad (1)$$

where $\boldsymbol{A}_r$ is the reduced vector potential, and μ is the permeability of the aluminum plate. Instead of moving the aluminum plate, z_{GAP} is time-dependent and the velocity term is not required in (1).

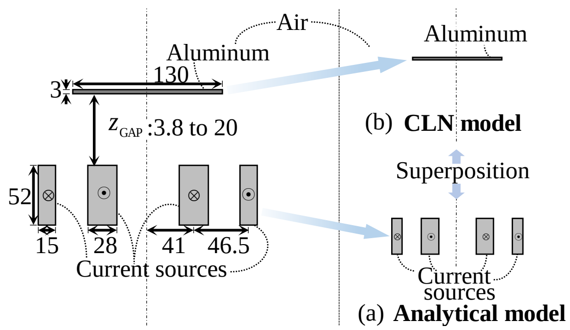

Fig. 1: Model geometry of TWP28. Dimensions are in millimeters. The problem is decomposed into two parts. The solutions of each model are superposed to reconstruct the solution of the original problem.

The procedure, discussed in [6] and [8], is employed to obtain the circuit parameters R_{2n}, L_{2n+1}, and the two sets of the basis functions $\hat{\boldsymbol{j}}_{2n}$, and $\hat{\boldsymbol{a}}_{2n}$ ($\hat{\boldsymbol{a}}_{2n}=\hat{\boldsymbol{a}}_{2n-1}-\hat{\boldsymbol{a}}_{2n+1}$) with the fixed levitaion height $z_{\mathrm{GAP}}=z_0$ and fixed time $t=t_0$. $\hat{\boldsymbol{a}}_{2n}$ act as the basis functions and $\hat{\boldsymbol{j}}_{2n}$ as the test functions. By testing the first term in (1) with $\hat{\boldsymbol{j}}_{2n}$, we obtain diagonal resistance matrix $\mathbf{R}$ whose coefficients are

$$R_{n,m}=\int_C\hat{\boldsymbol{j}}_{2n}\cdot\frac{1}{\sigma}\nabla\times\left(\frac{1}{\mu}\nabla\times\hat{\boldsymbol{a}}_{2m}\right)dV. \quad (2)$$

where C is a conducting domain. By testing the second term in (1), we obtain tridiagonal inductance matrix $\mathbf{L}$ whose coefficients are

$$L_{n,m}=\int_C\hat{\boldsymbol{j}}_{2n}\cdot\hat{\boldsymbol{a}}_{2m}dV. \quad (3)$$

We can derive the conventional CLN equation

$$\left(\mathbf{R}+\frac{\partial}{\partial t}\mathbf{L}\right)\begin{bmatrix} j_0\\ j_2\\ \vdots\\ j_{2N}\\ \vdots\end{bmatrix}=-\frac{\partial}{\partial t}\begin{bmatrix} a_{s0}(z_{\mathrm{gap}}=z_0,t)\\ 0\\ \vdots\\ 0\\ \vdots\end{bmatrix} \quad (4)$$

where j_{2n} are the coefficients of $\hat{\boldsymbol{j}}_{2m}$ and a_{s0} is a time-dependect coefficient of $\boldsymbol{A}_s(t)=a_{s0}(t)\boldsymbol{A}_s(t=t_0)$.

By testing the right-hand side in (1), $\boldsymbol{A}_s(z_{\mathrm{gap}})$ can be expanded with $\hat{\boldsymbol{j}}_{2n}$ as follows.

$$\boldsymbol{A}_s(z_{\mathrm{gap}}(t))\approx\sum_n a_{s2n}(z_{\mathrm{gap}}(t))\hat{\boldsymbol{j}}_{2n} \quad (5)$$

$$a_{s2n}(t)=\frac{1}{R_{2n}}\int_C\frac{\hat{\boldsymbol{j}}_{2n}\cdot\boldsymbol{A}_s(z_{\mathrm{gap}}(t),t)}{\sigma}dV \quad (6)$$

The dependence of the expansion coefficient $a_{2n}(z_{\mathrm{gap}})$ on z_{gap} is shown in Fig. 2 when z_0= 3.8mm. When z_{gap}=3.8 mm, $a_0=1$, $a_n=0$ for $n>0$, but as z_{gap} increases, a_0 decreases and a_n for $n>0$ increases. Fig. 3 shows comparisons of the vector potential $\boldsymbol{A}_s(z_{\mathrm{GAP}},t=t_0)$ reconstructed by (5) and that induced by the coils. It can be confirmed that the reproducibility increases as the expansion order increases.

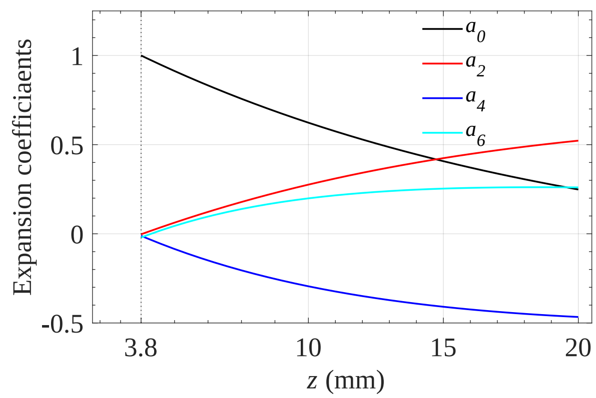

Fig. 2: z_{gap} dependence of the expansion coefficients

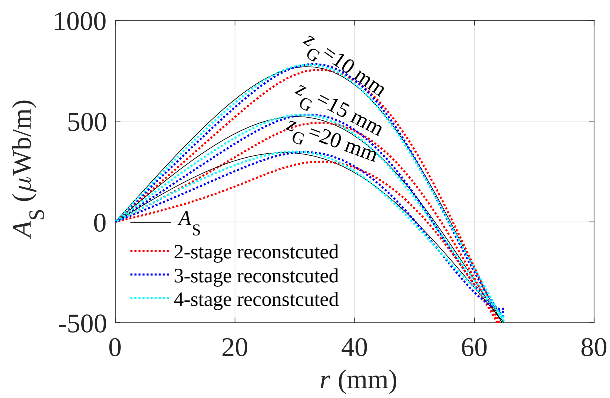

Fig. 3: $\boldsymbol{A}_s$ reconstructed by (5) The reproducibility increases as the expansion order increases.

There is no guarantee that $\boldsymbol{A}_s$ exists inside the space spanned by $\hat{\boldsymbol{j}}_{2n}$. Thus, if (5) is not a good approximation, the space must be expanded with an additional set of basis functions. For the case of motion involving only one direction, as in TWP28, (5) is a sufficient approximation.

With $\hat{\boldsymbol{a}}_{2n}$ and $\hat{\boldsymbol{j}}_{2n}$, we can discretize (1) to derive (7) for any value of z_{gap}. This is a natural extension of the conventional CLN method. The idea of the proposed CLN method is that the CLN on the left-hand side is constant by imposing the right-hand side to vary with the mover motion.

$$\left(\mathbf{R}+\frac{\partial}{\partial t}\mathbf{L}\right)\begin{bmatrix} i_0 \\ i_2 \\ \vdots \\ i_{2N} \\ \vdots \end{bmatrix} = -\frac{\partial}{\partial t}\begin{bmatrix} a_{s0}(z_{\text{gap}}(t),t) \\ a_{s2}(z_{\text{gap}}(t),t) \\ \vdots \\ a_{s2N}(z_{\text{gap}}(t),t) \\ \vdots \end{bmatrix} \tag{7}$$

The right-hand side of (7) corresponds to the voltage source on each stage of the CLN whereas the conventional CLN has only one voltage source at the first stage. Those voltage sources are modeled as a current-controlled voltage source, whose gains the opposite of the time derivatives of the expansion factors of $a_{s2n}(z_{\text{gap}}(t),t)$. The proposed CLN representation corresponding to (7) is shown in Fig. 4.

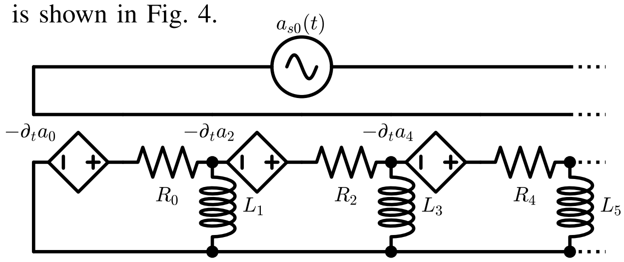

Fig. 4: Proposed CLN representation of TWP28.

III. Sinusoidal steady state analysis

We have construced the CLN with z_0= 3.8mm. The computational time of generating the 4-stage CLN model was approximately 30 s. The mover was fixed at a constant height of $z_{\text{gap}} = 20$ mm, and a sinusoidal steady-state analysis was performed at f =50 Hz. Fig. 5 shows the comparison of the eddy current distributions at the center of the aluminum plate. (a) and (f) are the results of FEM and others are differencies between the proposed CLN method and FEM with various stages. It can be seen that the error decreases for both the real and imaginary parts as the expansion order increases.

Fig. 6 shows the comparison of the time-averaged Lorentz force in the sinusoidal steady state with the FEM. The FEM results are already sufficiently reproduced with 2-stages CLN and the results do not change even if the expansion order is increased thereafter.

Fig. 7 shows the comparison of the Joule loss in the sinusoidal steady state with the FEM. The FEM results are already sufficiently reproduced with 2-stages CLN and the results do not change even if the expansion order is increased thereafter.

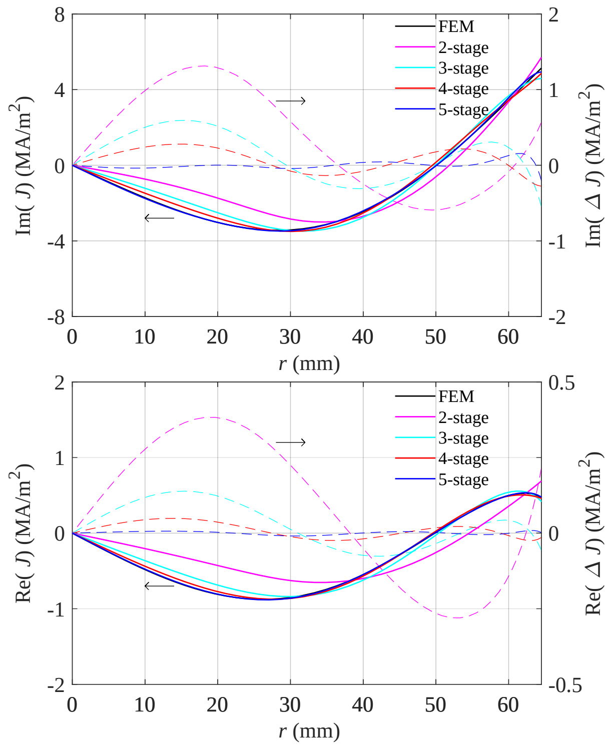

Fig. 5: Eddy current density obtained by FEM and the proposed CLN, and those two differences.

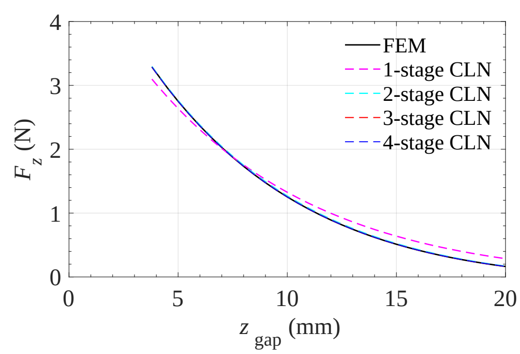

Fig. 6: z_{gap} dependence of the time-averaged force

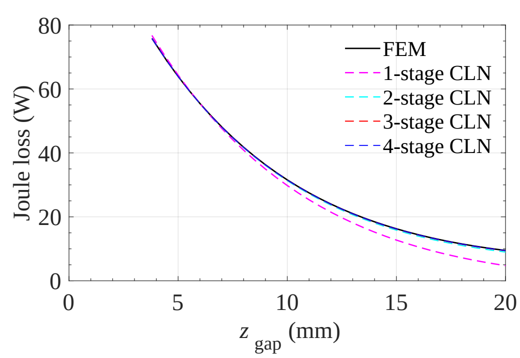

Fig. 7: z_{gap} dependence of the Joule loss

IV. Transient analysis coupled with motion

Fig. 8 shows a block diagram of the proposed CLN method implemented in Simulink for motion coupling. The width of the time step Δt was set to 0.1 ms and simulations were performed for 20,000 steps from 0 ms to 2000 ms. We observed $\Delta t = 1.0$ ms was too large and it must be smaller than $\Delta t = 0.5$ ms at least. The environment used for the calculations was Intel Core i5-12400 CPU, 64GB memory. Fig. 9 shows a comparison of the measured magnetic levitation height [12], that obtained by the commercial software (ELF/MAGIC), and the proposed method. The fine oscillations with a period of 20 ms, which appear among the large periodic damped oscillations with a period of 200 ms, are considered to be caused by the power supply frequency of 50 Hz. The results of the 2-stage CLN reproduce the ELF/MAGIC's results with an error of less than a few percent. As for the actual measurement results, they are likely to contain some errors that differ from ideal electromagnetic field modeling. The proposed CLN method requires only about 5 s for transient analysis, which is a significant reduction in analysis time compared to the 40 min required by ELF/MAGIC.

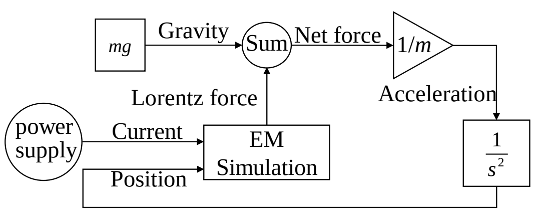

Fig. 8: Block diagram of the proposed CLN coupled with the equation of motion

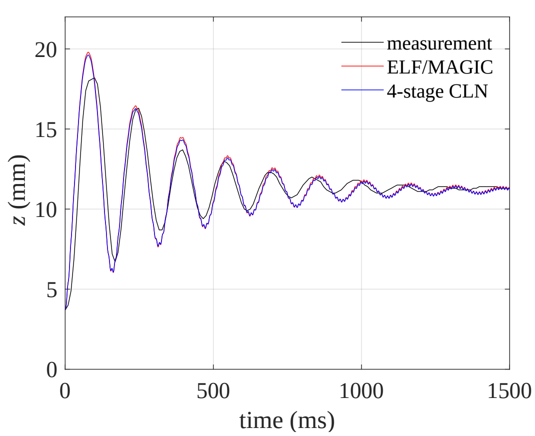

Fig. 9: Levitation height transients evaluated from measurements, commercial software, and proposed CLN approach

V. Conclusion

The CLN method with constant basis functions for eddy current problems involving translational movements has been proposed. Because both the circuit parameters and the basis functions are constant, the implementation on the circuit simulator is simple and analysis can be easily performed with circuit simulators used for control design. To show the validity of the proposed method, an analysis of the TWP 28 was performed and the computation time has been significantly reduced without the loss of accurary. We plan to apply this method to cases where multiple conductors exist.

Acknowledgment

This work was supported by JSPS KAKENHI (Grant-in-Aid for Scientific Research (C)) Grant Number JP20K04454.

References

[1] K. Hollaus and J. Schoberl, "Some 2-D multiscale finite-element formulations for the eddy current problem in iron laminates," *IEEE Trans. Magn.*, vol. 54, no. 4, pp. 1–16, 2018.

[2] A. Pierquin, T. Henneron, S. Clenet, and S. Brisset, "Model-order reduction of magnetoquasi-static problems based on POD and Arnoldi-based Krylov methods," *IEEE Trans. Magn.*, vol. 51, no. 3, pp. 1–4, March 2015.

[3] T. Henneron and S. Clenet, "Model-order reduction of multiple-input non-linear systems based on POD and DEI methods," *IEEE Trans. Magn.*, vol. 51, no. 3, 2015.

[4] Y. Sato and H. Igarashi, "Model reduction of three-dimensional eddy current problems based on the method of snapshots," *IEEE Trans. Magn.*, vol. 49, no. 5, 2013.

[5] A. Kameari, H. Ebrahimi, K. Sugahara, Y. Shindo, and T. Matsuo, "Cauer ladder network representation of eddy-current fields for model order reduction using finite-element method," *IEEE Trans. Magn.*, vol. 54, no. 3, 2017.

[6] K. Sugahara, A. Kameari, H. Ebrahimi, Y. Shindo, and T. Matsuo, "Finite-element analysis of unbounded eddy-current problems using Cauer ladder network method," *IEEE Trans. Magn.*, vol. 54, no. 3, 2017.

[7] K. Kuriyama, A. Kameari, H. Ebrahimi, T. Fujiwara, K. Sugahara, Y. Shindo, and T. Matsuo, "Cauer ladder network with multiple expansion points for efficient model order reduction of eddy-current field," *IEEE Transactions on Magn.*, vol. 55, no. 6, pp. 1–4, June 2019.

[8] S. Hiruma and H. Igarashi, "Model order reduction for linear time-invariant system with symmetric positive-definite matrices: Synthesis of Cauer-equivalent circuit," *IEEE Trans. Magn.*, vol. 56, no. 3, 2020.

[9] N. Koster, O. Konig, and O. Biro, "Proper generalized decomposition with Cauer ladder network applied to eddy current problems," *IEEE Trans. Magn.*, vol. 57, no. 6, pp. 1–4, 2021.

[10] Y. Shindo, R. Yamamoto, K. Sugahara, T. Matsuo, and A. Kameari, "Equivalent circuit in Cauer form for eddy current field including a translational mover," *IEEE Trans. Magn.*, vol. 56, no. 12, pp. 1–7, 2020.

[11] R. V. Sabariego, B. Vanbroekhoven, J. Gyselinck, and P. Kuo-Peng, "RL-Ladder circuit models for eddy-current problems with translational movement," *IEEE Trans. Magn.*, vol. 58, no. 9, pp. 1–4, 2022.

[12] H. Karl, J. Fetzer, S. Kurz, G. Lehner, and W. M. Rucker, "Description of TEAM Workshop Problem 28: An electrodynamic levitation device," *Proc. of the TEAM Workshop, Graz, Austria.*

[13] S.-M. Lee, S.-H. Lee, H.-S. Choi, and I.-H. Park, "Reduced modeling of eddy current-driven electromechanical system using conductor segmentation and circuit parameters extracted by FEA," *IEEE Trans. Magn.*, vol. 41, no. 5, pp. 1448–1451, 2005.

[14] T. Matsuo, A. Kameari, K. Sugahara, and Y. Shindo, "Matrix formulation of the Cauer ladder network method for efficient eddy-current analysis," *IEEE Transactions on Magn.*, vol. 54, no. 11, pp. 1–5, Nov 2018.